CHAPTER 3

SYNTHESIS AND CHARACTERIZATION OF TIN(II) ALKOXIDES

3.1 Tin(II) Alkoxides

Tin(II) alkoxides (or stannous alkoxides) are readily prepared by the method of Morrison and Haendler [62] (Eqn. 3.1) or by transesterification of $Sn(OCH_3)_2$ with a higher boiling alcohol (Eqn 3.2).

$$SnCl_2 + 2\,ROH + 2\,(C_2H_5)_3N \longrightarrow Sn(OR)_2 + 2\,(C_2H_5)_3N.HCl \qquad (3.1)$$

$$Sn(OCH_3)_2 + 2\,ROH \longrightarrow Sn(OR)_2 + 2\,CH_3OH \qquad (3.2)$$

The lability of these compounds suggests their potential as important reaction intermediates in tin(II) chemistry. Unfortunately, the scope of the chemistry of these compounds has not been fully explored and there have been relatively few reports of specific reactions [63]. The slow development of this field may well be linked to the paucity of property and structure information on these compounds as well as the fact that tin(II) alkoxides have low solubilities in organic solvents and are sensitive to oxygen and moisture.

3.2 Purification of Reagents

Because trace amounts of moisture and other impurities could be present in the reagents used in this research project, they required further purification. As mentioned above, tin(II) alkoxides are both moisture and air-sensitive and so their synthesis needs to be carried out using pure reagents in an inert atmosphere.

3.2.1 Alcohols

In this research, each of the primary alcohols (ROH) used was purified by fractional distillation under atmospheric pressure (approx. 730 mm Hg) using the apparatus shown in Figure 3.1. The alcohol was first dried by refluxing over sodium metal to absorb moisture before distillation. After decanting the alcohol away from the drying agent, about 1 g/l of calcium hydride was added prior to distillation. In the distillation that followed, the pure alcohol was collected as the constant boiling fraction under a dry nitrogen atmosphere. The purified alcohol was stored in a vacuum desiccator until required for use in synthesis.

A list of the primary alcohols purified in this way is given in Table 3.1. The observed constant boiling point of each alcohol as collected is compared alongside the corresponding literature value.

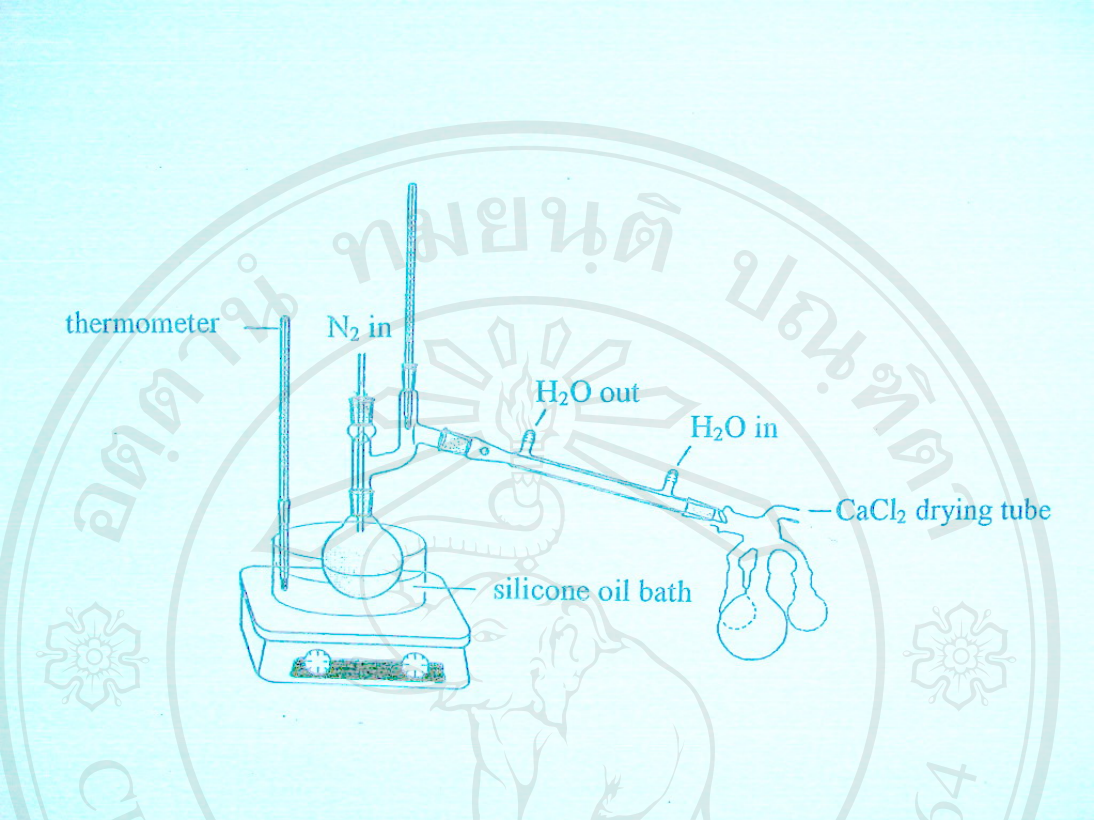

Figure 3.1 Fractional distillation apparatus used in the purification of the primary alcohols.

Table 3.1 Constant boiling points of the purified primary alcohols (ROH) obtained from the fractional distillations.

Primary Alcohol ROH	R	Grade * or Assay	Observed B.Pt. ** (^oC)	Literature B.Pt. *** (^oC)
Methanol	CH_3	Commercial	64	64
Ethanol	C_2H_5	Absolute	78	78-79
1-Propanol	C_3H_7	99 %	98	97
1-Butanol	C_4H_9	99.9 %	116	116-118
1-Hexanol	C_6H_{13}	> 98 %	157	156
1-Octanol	C_8H_{17}	99 %	194	196

* All were Merck products
** Constant boiling fraction at atmospheric pressure (730 mm Hg)
*** Literature values at 760 mm Hg pressure obtained from reference [79]

3.2.2 Triethylamine

Triethylamine (Ajax, assay 99 %) was also purified by fractional distillation at atmospheric pressure using a similar procedure and apparatus to that for the alcohols. The constant boiling fraction at 86 ^{o}C (cf. lit [79] 88.8 ^{o}C/760 mm Hg) was collected under a dry nitrogen atmosphere and then stored in a vacuum desiccator until required for use in synthesis.

3.2.3 Tin(II) Chloride

Anhydrous tin(II) chloride (stannous chloride), $SnCl_2$, was used as supplied (Acros Organics, 98 %) without further purification. Due to its hygroscopic nature, it was stored in a tightly sealed container in a vacuum desiccator. On exposure to air, anhydrous $SnCl_2$ readily absorbs moisture and converts to the much less reactive dihydrate, $SnCl_2.2H_2O$.

3.3 Synthesis and Purification of Tin(II) Alkoxides

A series of tin(II) alkoxides was prepared from the reaction of anhydrous $SnCl_2$ with the corresponding excess dry alcohols in the presence of triethylamine, as described by Morrison and Haendler [62]. In a typical experiment, approximately 6.0 g $SnCl_2$ were dissolved in a large excess of 125 ml dry alcohol in a 250 ml round-bottomed flask under a dry nitrogen atmosphere at room temperature (Figure 3.2). 10 ml triethylamine were then added with magnetic stirring to cause a permanent precipitate and stirring continued for a further 3 hrs. The precipitate was filtered, washed with more dry alcohol, then with diethyl ether and dried under vacuum at 60 ^{o}C. This solid product was a mixture of both the tin(II) alkoxide and the triethylamine hydrochloride by-product, according to the reaction below:

$$SnCl_2 + 2\,ROH + 2\,(C_2H_5)_3N \longrightarrow Sn(OR)_2 + 2\,(C_2H_5)_3N.HCl$$

The $Sn(OR)_2$ was separated from the hydrochloride by-product by solvent extraction. The mixture was stirred in (distilled) chloroform at 40 ^{o}C for 3 hrs in order to dissolve the soluble hydrochloride. The insoluble $Sn(OR)_2$ was then filtered off in a dry box, washed with more chloroform, and dried to constant weight in a vacuum oven at 60 ^{o}C. Finally, due to their sensitivity towards oxygen and moisture, the $Sn(OR)_2$ products were stored under nitrogen in tightly sealed containers in a vacuum desiccator until required for use. The physical appearances and % yields of all of the purified $Sn(OR)_2$ products are given in Table 3.2.

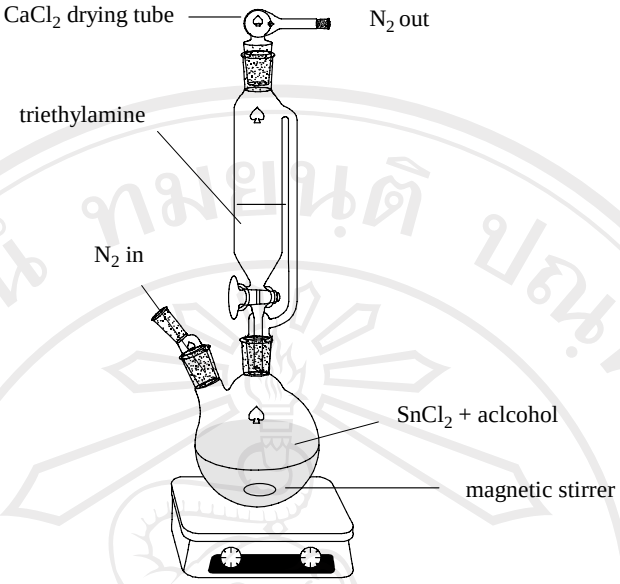

Figure 3.2 Apparatus used for the synthesis of the tin(II) alkoxides.

Table 3.2 Physical appearances and % yields of the purified $Sn(OR)_2$ products.

Tin(II) Alkoxide	Molecular Formula	Physical Appearance	% Yield
Tin(II) methoxide	$Sn(OCH_3)_2$	White solid powder	90.9
Tin(II) ethoxide	$Sn(OC_2H_5)_2$	White solid powder	85.3
Tin(II) propoxide	$Sn(OC_3H_7)_2$	White solid powder	79.3
Tin(II) butoxide	$Sn(OC_4H_9)_2$	White solid powder	26.2
Tin(II) hexoxide	$Sn(OC_6H_{13})_2$	White solid powder	10.6
Tin(II) octoxide	$Sn(OC_8H_{17})_2$	White solid powder	9.3

As seen in Table 3.2, the % yield of the $Sn(OR)_2$ decreased dramatically when $R > C_3H_7$. It is significant to note here that, in their preparation of $Sn(OC_4H_9)_2$, Gsell and Zeldin [63] used an alternative method involving transalkoxidation of $Sn(OCH_3)_2$ with 1-butanol in toluene, as represented by the equation:

$$Sn(OCH_3)_2 + 2C_4H_9OH \longrightarrow Sn(OC_4H_9)_2 + 2\,CH_3OH$$

Strangely, no explanation was given in Gsell and Zeldin's paper as to why this transalkoxidation method was preferred over the direct reaction of 1-butanol with $SnCl_2$ for higher alkoxides. However, when this transalkoxidation method was used in this work to prepare $Sn(OC_4H_9)_2$, the reaction did not proceed as described by Gsell and Zeldin. Instead, $Sn(OCH_3)_2$ remained undissolved in the refluxing toluene, even after prolonged (several days) heating with stirring, and no reaction with the 1-butanol in solution occurred. Consequently, all of the alkoxides synthesized in this work were synthesized via the direct reactions of the alcohols with $SnCl_2$ even though the yields (Table 3.2) for R > C_3H_7 were drastically reduced. The reason(s) for these reduced yields is still uncertain since the conditions of this $Sn(OR)_2$ synthesis reaction were not studied in detail. It can only be assumed that the greatly reduced yields for R > C_3H_7 is a consequence of kinetic and/or thermodynamic factors. This would be an interesting topic for further study.

3.4 Characterization of Tin(II) Alkoxides

In this work, characterization of the tin(II) alkoxides (solubility, chemical structure, temperature transitions and thermal stability) were carried out via the following combination of analytical techniques:

- Solubility testing
- Fourier-transform infrared spectroscopy (FT-IR)
- Raman spectroscopy
- Carbon-13 nuclear magnetic resonance spectroscopy (^{13}C-NMR)
- Differential scanning calorimetry (DSC)
- Thermogravimetric analysis (TGA)

Except for solubility testing, each of these techniques, including the instrument used, was described previously in section 2.3 (Instrumental Methods) of this thesis.

3.4.1 Solubility Testing

The following procedure was used for the determination of solubility. A small amount of the tin(II) alkoxide was mixed with 10.0 ml of solvent in a 25 ml stopped conical flask and stirred together thoroughly. If no sign of solubility occurred at room temperature, the mixture was heated at a temperature just below the boiling point of the solvent. Various solvents were tested in this way and the solubility test results are shown in Table 3.3.

The results in Table 3.3 confirm the difficult solubility of the tin(II) alkoxides. At most, they were only partially soluble in hot, high boiling point polar solvents such as dimethyl sulphoxide (DMSO) and *o*-dichlorobenzene. This difficult solubility is

attributed to molecular aggregation in the solid state forming “polymeric” species of the types shown below [63]. This aggregation is driven by the availability of empty valence ‘d’ orbitals on the Sn atoms.

Molecular aggregation in tin(II) alkoxides

Table 3.3 Solubility test results for the tin(II) alkoxides.

Tin(II) Alkoxide / Solvent	Tin(II) Methoxide	Tin(II) Ethoxide	Tin(II) Propoxide	Tin(II) Butoxide	Tin(II) Hexoxide	Tin(II) Octoxide
Methanol	X	X	X	X	X	X
Ethanol	X	X	X	X	X	X
Acetone	X	X	X	X	X	X
Chloroform	X	X	X	X	X	X
Toluene	X	X	X	X	X	X
Dimethyl Sulfoxide	X	X	δ	δ	δ	δ
o-Dichlorobenzene	X	X	δ	δ	δ	δ

Notations: X = insoluble, even on prolonged heating
δ = partially soluble on heating

3.4.2 Fourier-Transform Infrared Spectroscopy (FT-IR)

The FT-IR spectra of the purified tin(II) alkoxides are shown in Figures 3.3-3.8. The samples for FT-IR analysis were prepared in the form of KBr discs. The major vibrational peak assignments are listed in Tables 3.4-3.9.

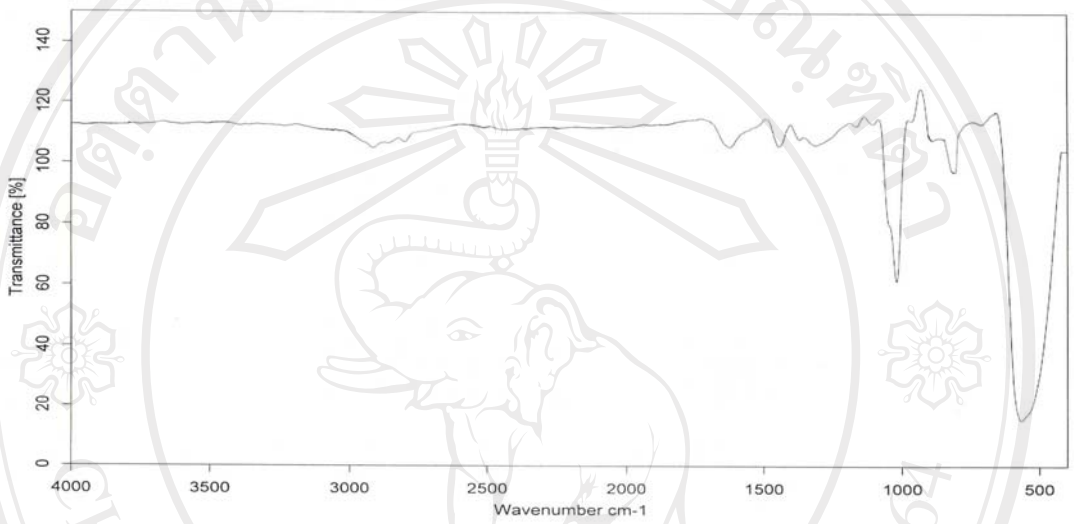

Figure 3.3 FT-IR spectrum of tin(II) methoxide.

Table 3.4 FT-IR absorption band assignments for tin(II) methoxide.

Vibrational Assignment	Wavenumber (cm^{-1})
C-H stretching	2882-2794
C-H bending	1426
C-O stretching	1015
Sn-O-Sn stretching in SnO_2Sn	809
Sn-O stretching	560

Chemical Structure (Monomeric)

$$CH_3—O—Sn—O—CH_3$$

tin(II) methoxide

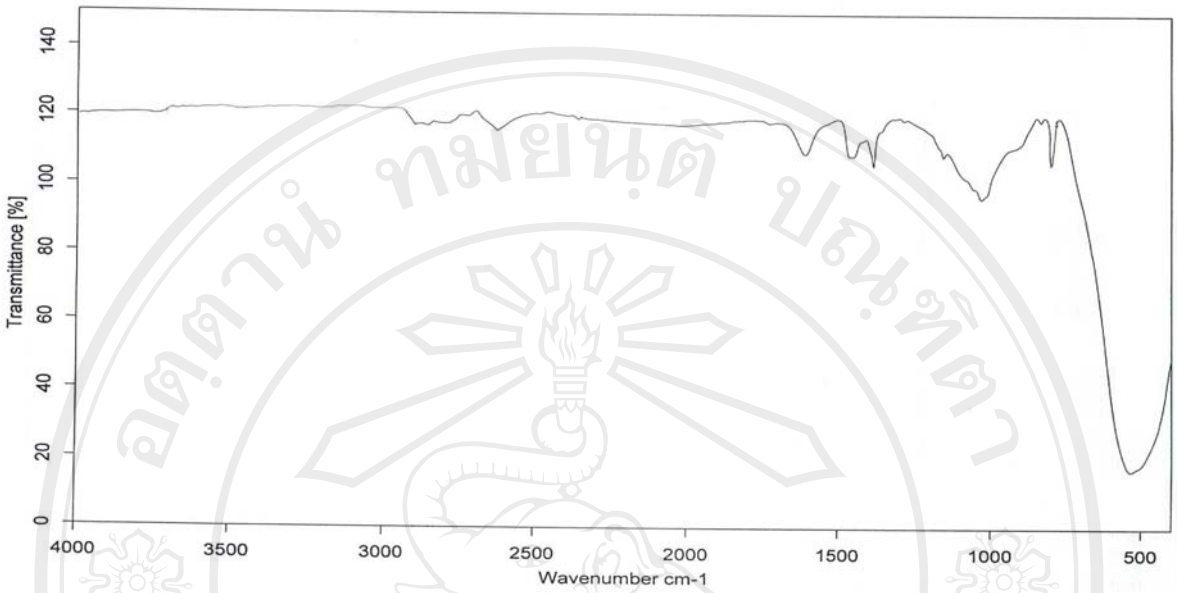

Figure 3.4 FT-IR spectrum of tin(II) ethoxide.

Table 3.5 FT-IR absorption band assignments for tin(II) ethoxide.

Vibrational Assignment	Wavenumber (cm^{-1})
C-H stretching	2838-2897
C-H bending	1455, 1382
C-O stretching	1015
Sn-O-Sn stretching in SnO_2Sn	809
Sn-O stretching	530

Chemical Structure (Monomeric)

$$CH_3—CH_2—O—Sn—O—CH_2—CH_3$$

tin(II) ethoxide

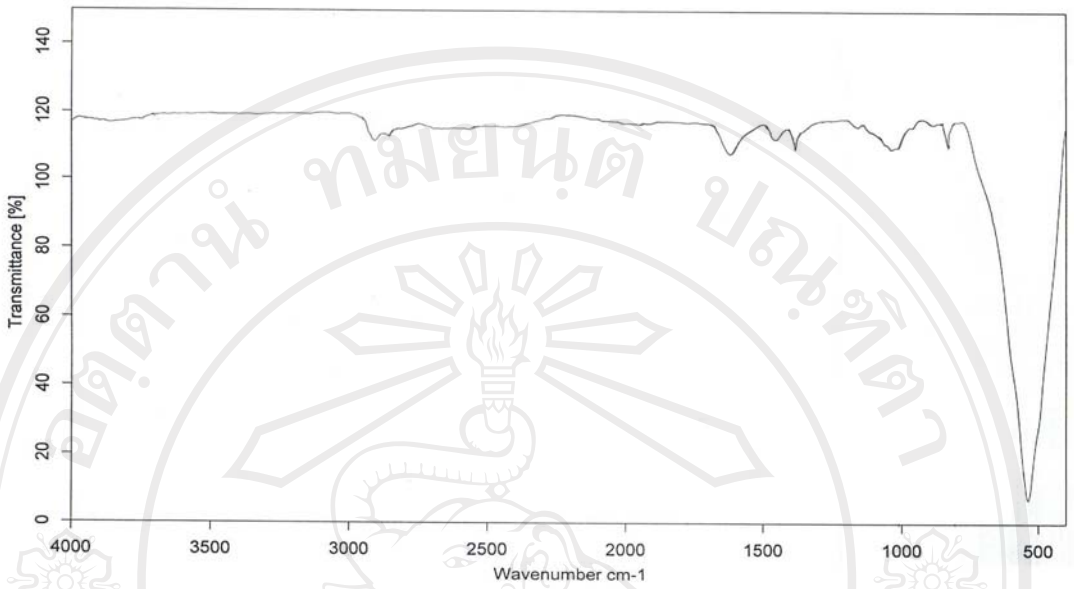

Figure 3.5 FT-IR spectrum of tin(II) propoxide.

Table 3.6 FT-IR absorption band assignments for tin(II) propoxide.

Vibrational Assignment	Wavenumber (cm^{-1})
C-H stretching	2838-2882
C-H bending	1456, 1382
C-O stretching	1015
Sn-O-Sn stretching in SnO_2Sn	809
Sn-O stretching	530

Chemical Structure (Monomeric)

$$CH_3—CH_2—CH_2—O—Sn—O—CH_2—CH_2—CH_3$$

tin(II) propoxide

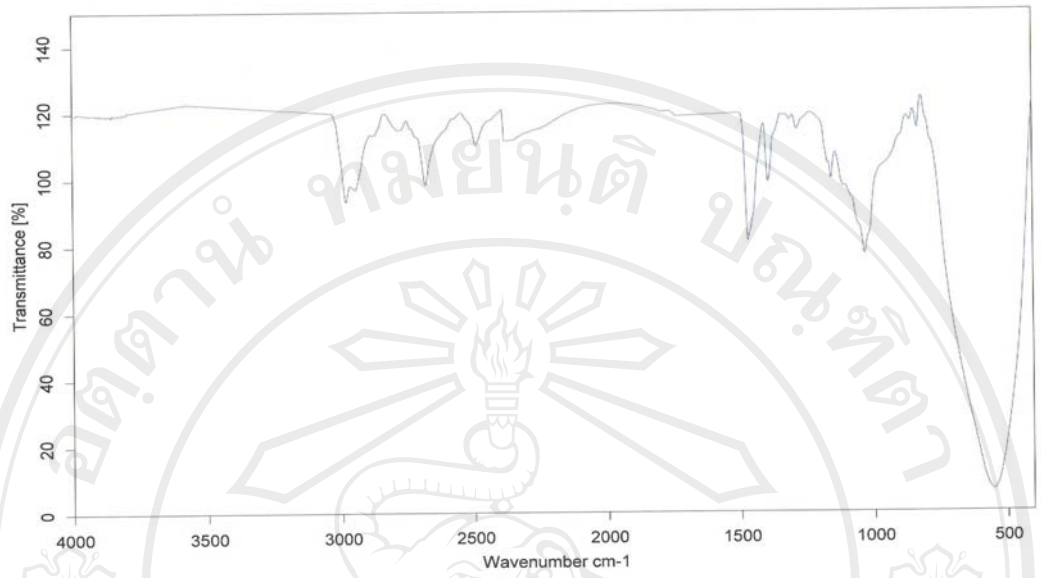

Figure 3.6 FT-IR spectrum of tin(II) butoxide.

Table 3.7 FT-IR absorption band assignments for tin(II) butoxide.

Vibrational Assignment	Wavenumber (cm^{-1})
C-H stretching	2941-2970
C-H bending	1470, 1382
C-O stretching	1015
Sn-O-Sn stretching in SnO_2Sn	809
Sn-O stretching	544

Chemical Structure (Monomeric)

$$CH_3—CH_2—CH_2—CH_2—O—Sn—O—CH_2—CH_2—CH_2—CH_3$$

tin(II) butoxide

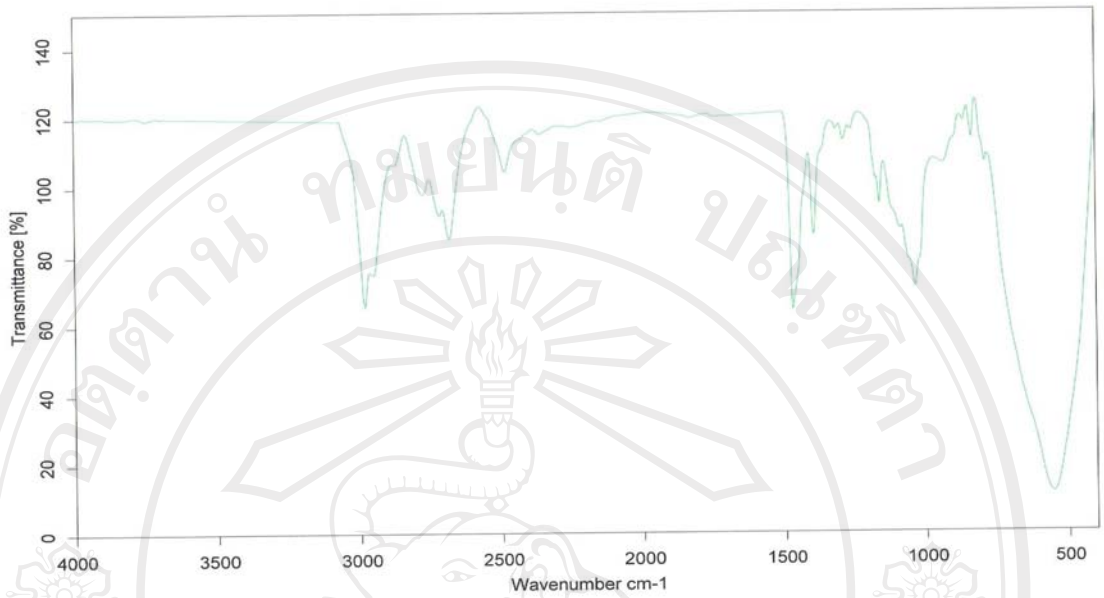

Figure 3.7 FT-IR spectrum of tin(II) hexoxide.

Table 3.8 FT-IR absorption band assignments for tin(II) hexoxide.

Vibrational Assignment	Wavenumber (cm^{-1})
C-H stretching	2941-2970
C-H bending	1456, 1382
C-O stretching	1015
Sn-O-Sn stretching in SnO_2Sn	809
Sn-O stretching	544

Chemical Structure (Monomeric)

$CH_3—CH_2—CH_2—CH_2—CH_2—CH_2—O—Sn—O—CH_2—CH_2—CH_2—CH_2—CH_2—CH_3$

tin(II) hexoxide

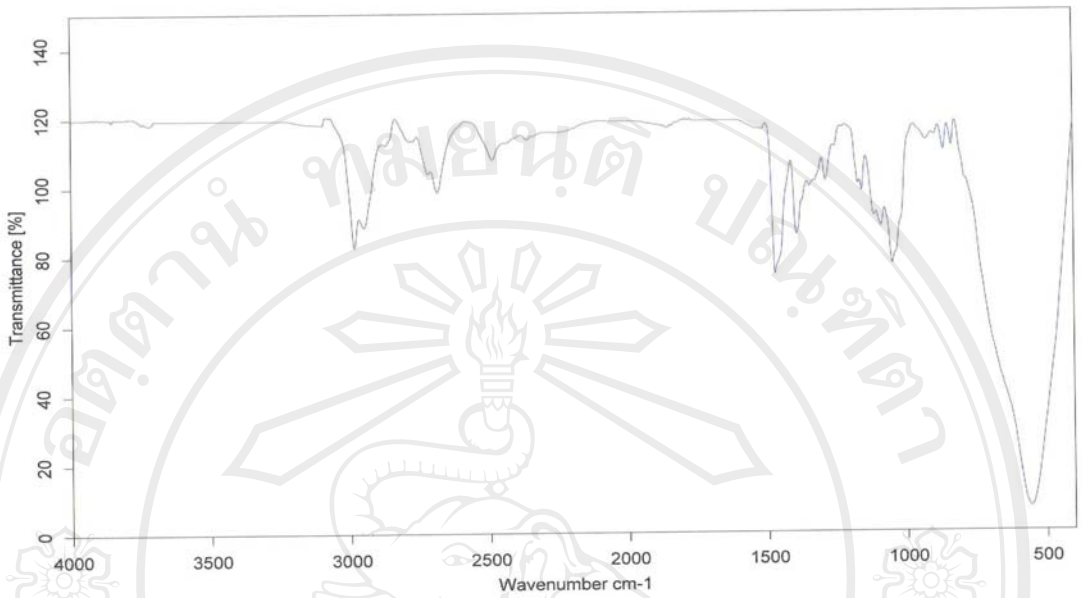

Figure 3.8 FT-IR spectrum of tin(II) octoxide.

Table 3.9 FT-IR absorption band assignments for tin(II) octoxide.

Vibrational Assignment	Wavenumber (cm^{-1})
C-H stretching	2941-2970
C-H bending	1470, 1382
C-O stretching	1015
Sn-O-Sn stretching in SnO_2Sn	815
Sn-O stretching	544

Chemical Structure (Monomeric)

$CH_3-CH_2-CH_2-CH_2-CH_2-CH_2-CH_2-CH_2-O-Sn-O-CH_2-CH_2-CH_2-CH_2-CH_2-CH_2-CH_2-CH_3$

tin(II) octoxide

In general, the FT-IR spectra in Figs. 3.3-3.8 are consistent with the chemical structures of the tin(II) alkoxides. It is noticeable in the spectra that peak resolution improves as the size of the R group increases. For R = CH_3, C_2H_5 and C_3H_7, the C-H bond vibrations associated with the R group are very weak compared with the intense Sn-O bond vibration. However, for R = C_4H_9, C_6H_{13} and C_8H_{17}, the C-H stretching and bending vibrations are much more visible. A possible explanation for this is that, for R > C_3H_7, the degree and/or strength of molecular aggregation decreases, thereby allowing the bonds in the OR groups to vibrate more freely. Interestingly, the previous solubility test results in Table 3.3 showed a similar trend. Since solubility would also be expected to increase with decreasing aggregation, the FT-IR and solubility results can be considered to be reflective in different ways of the same effect of the state of aggregation.

In support of these conclusions, it should also be mentioned here that the FT-IR spectrum of triethylamine hydrochloride (Fig. 3.9), the by-product from the tin(II) alkoxide syntheses, is quite different from the spectra of the tin(II) alkoxides. The absence of any characteristic peaks of triethylamine hydrochloride in the tin(II) alkoxide spectra serves to confirm that it was completely removed during the purification process by chloroform extraction.

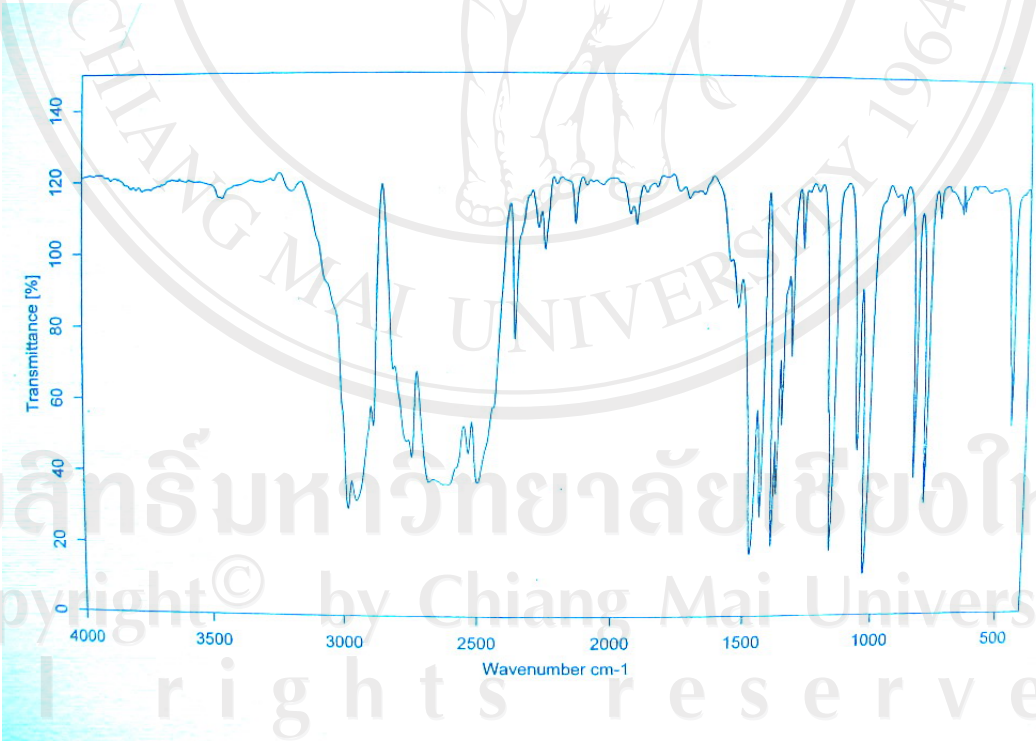

Figure 3.9 FT-IR spectrum of triethylamine hydrochloride, $(C_2H_5)_3N.HCl$ (Commercial product: Sigma).

3.4.3 Raman Spectroscopy

As mentioned in the previous chapter, Raman spectroscopy can be considered to be complementary to infrared spectroscopy. Even though the two techniques provide similar information, Raman spectroscopy has certain advantages which are particularly relevant to the analysis of tin(II) alkoxides, most notably:

(1) it is more amenable to the study of solid samples in powder form
(2) it routinely analyses down to frequencies of below 400 cm^{-1}, a region in which Sn-O bonds are vibrationally active

The Raman scattering spectra of the tin(II) alkoxides are shown in Figures 3.10-3.15 and the vibrational assignments listed in Tables 3.10-3.15. The spectra were obtained from solid samples ground into fine powders and contained between quartz glass slides.

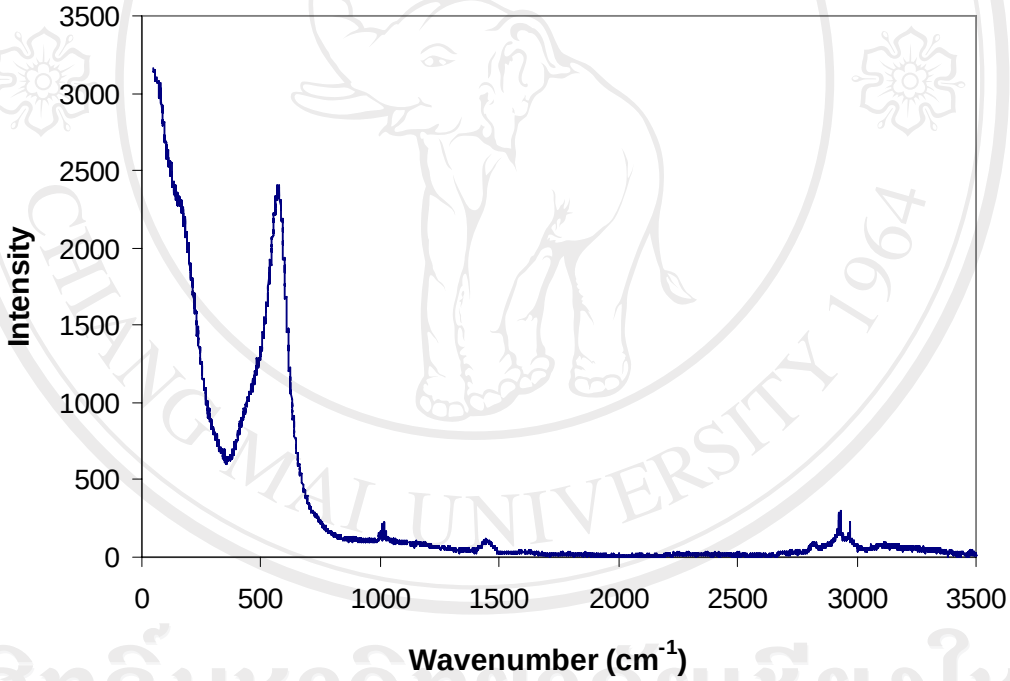

Figure 3.10 Raman scattering spectrum of tin(II) methoxide.

Table 3.10 Vibrational assignments in the Raman spectrum of tin(II) methoxide.

Vibrational Assignment	Wavenumber (cm^{-1})
C-H stretching in CH_3 C-H bending in CH_3 C-O stretching Sn-O stretching	2930-2970 1446 1015 576

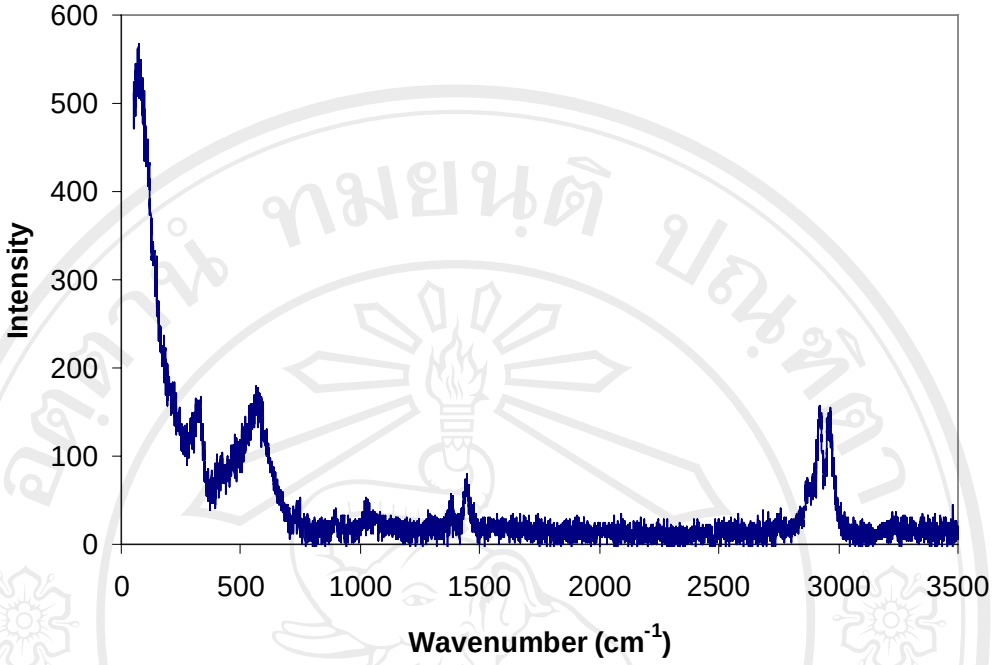

Figure 3.11 Raman scattering spectrum of tin(II) ethoxide.

Table 3.11 Vibrational assignments in the Raman spectrum of tin(II) ethoxide.

Vibrational Assignment	Wavenumber (cm^{-1})
C-H stretching in CH_2, CH_3	2964-2920
C-H bending in CH_2, CH_3	1445, 1381
C-O stretching	1025
Sn-O stretching	577
Sn-O-Sn stretching	330

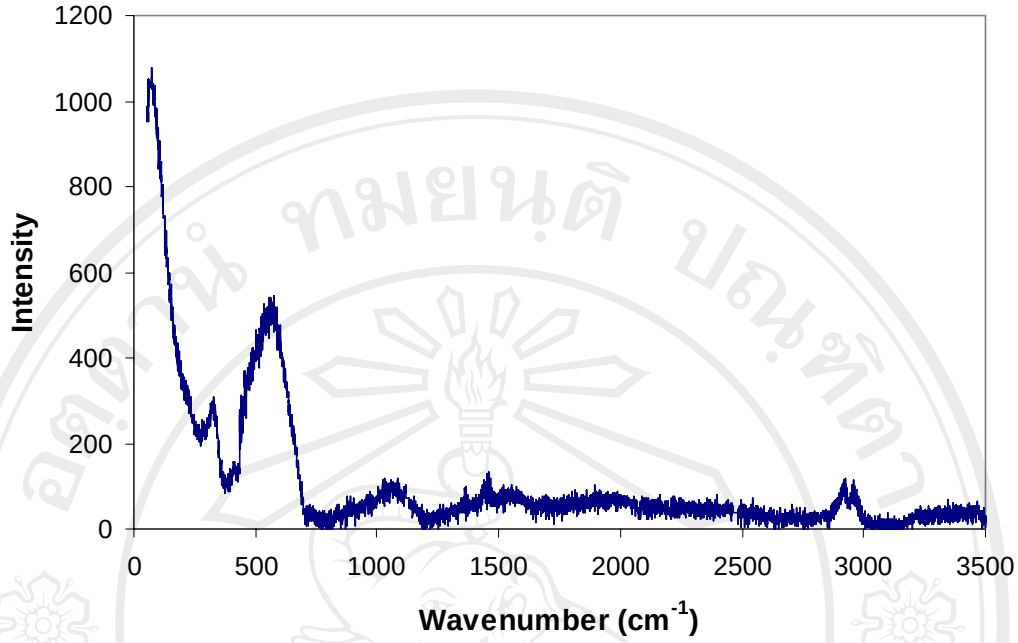

Figure 3.12 Raman scattering spectrum of tin(II) propoxide.

Table 3.12 Vibrational assignments in the Raman spectrum of tin(II) propoxide.

Vibrational Assignment	Wavenumber (cm^{-1})
C-H stretching in CH_2, CH_3	2922-2960
C-H bending in CH_2, CH_3	1456, 1367
C-O stretching	1020
Sn-O stretching	576
Sn-O-Sn stretching	329

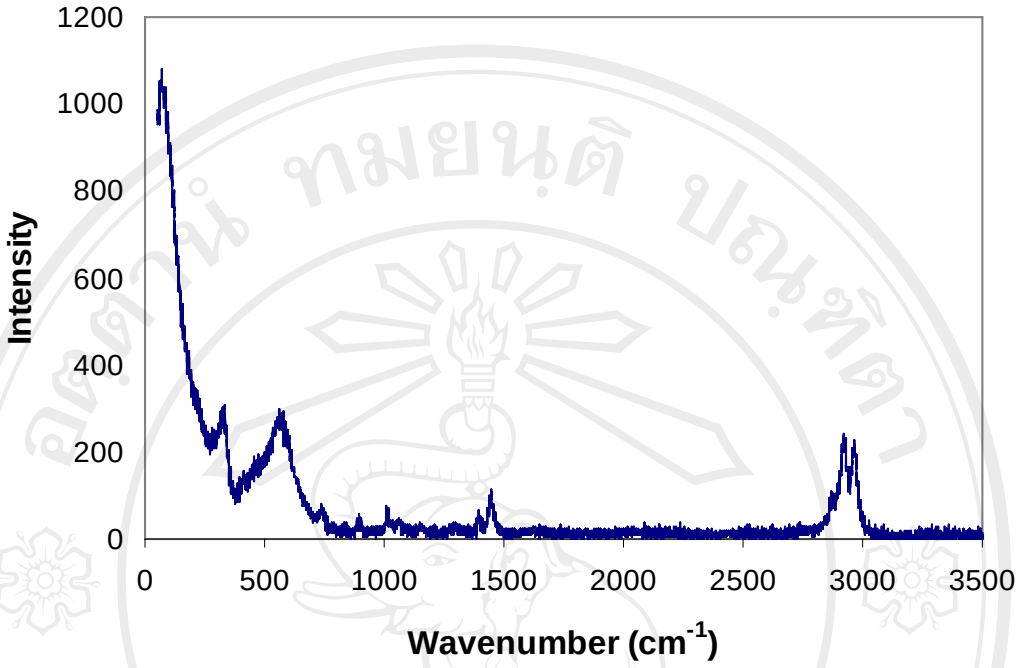

Figure 3.13 Raman scattering spectrum of tin(II) butoxide.

Table 3.13 Vibrational assignments in the Raman spectrum of tin(II) butoxide.

Vibrational Assignment	Wavenumber (cm^{-1})
C-H stretching in CH_2, CH_3	2965-2925
C-H bending in CH_2, CH_3	1449, 1394
C-O stretching	1012
Sn-O stretching	576
Sn-O-Sn stretching	329

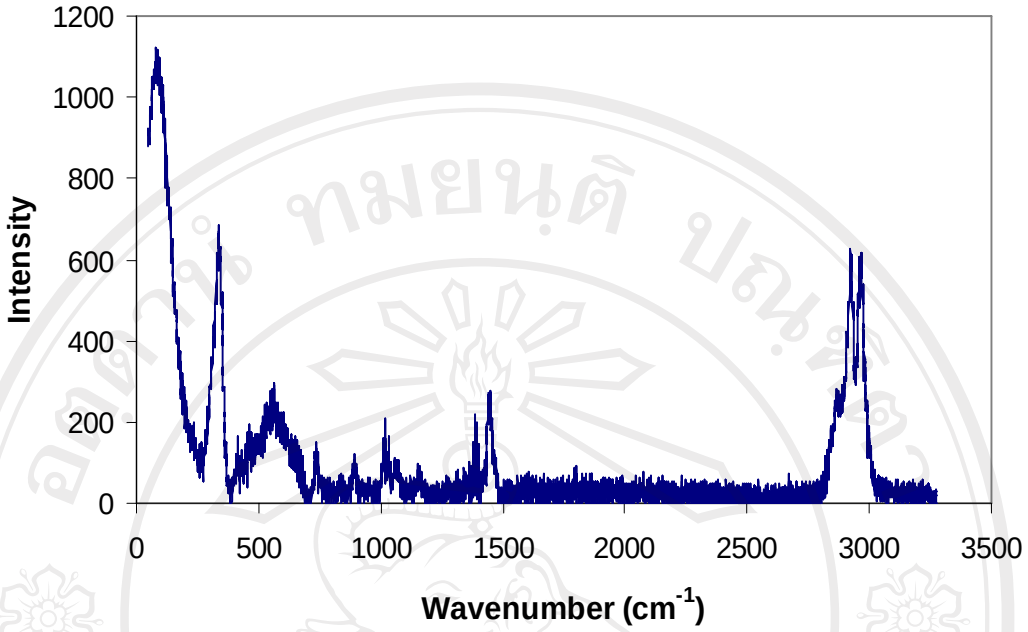

Figure 3.14 Raman scattering spectrum of tin(II) hexoxide.

Table 3.14 Vibrational assignments in the Raman spectrum of tin(II) hexoxide.

Vibrational Assignment	Wavenumber (cm^{-1})
C-H stretching in CH_2, CH_3	2967-2927
C-H bending in CH_2, CH_3	1450, 1380
C-O stretching	1015
Sn-O stretching	566
Sn-O-Sn stretching	339

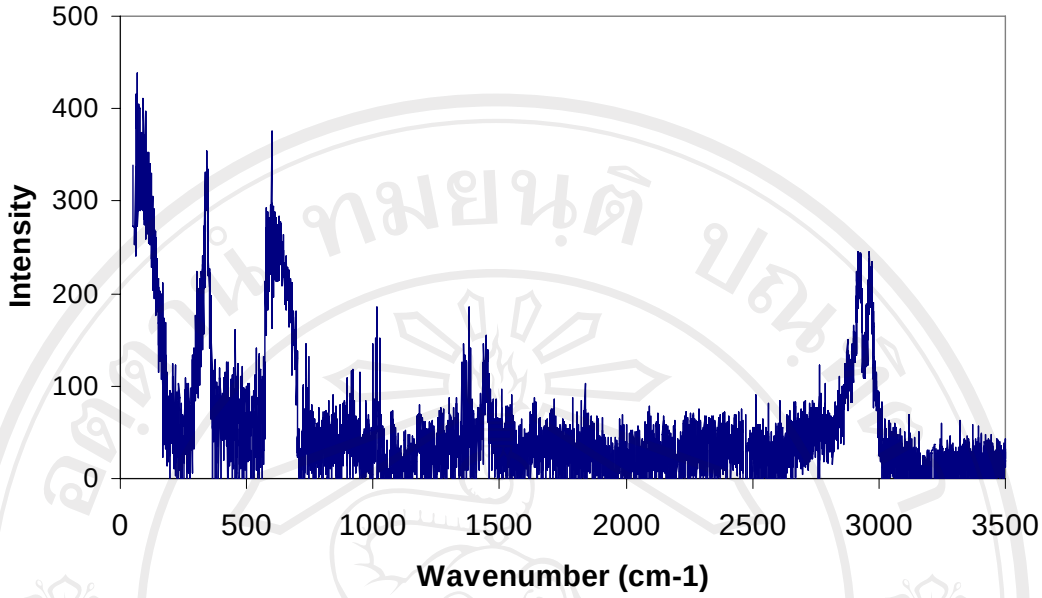

Figure 3.15 Raman scattering spectrum of tin(II) octoxide.

Table 3.15 Vibrational assignments in the Raman spectrum of tin(II) octoxide.

Vibrational Assignment	Wavenumber (cm^{-1})
C-H stretching in CH_2, CH_3	2964-2927
C-H bending in CH_2, CH_3	1448, 1380
C-O stretching	1015
Sn-O stretching	598
Sn-O-Sn stretching	344

Although the Raman spectra are consistent with the previous FT-IR spectra and therefore lend further support to the structural characterization, they are not as well resolved as expected. Indeed, their resolution is less than the FT-IR spectra. The reason(s) for this is unclear but it is considered that resolution could be improved by a more detailed study of the sample preparation and scanning conditions.

It is interesting to note that the Raman spectra, in common with the FT-IR spectra, show improved resolution for the higher alkoxides. Figures 3.14 and 3.15 for the hexoxide and octoxide show significantly stronger absorptions which support the previous view that they are less aggregated. This molecular aggregation hinders their structural characterization due to the restrictions which it imposes on molecular motion. Presumably, this is the main reason for the paucity of spectroscopic data for tin(II) alkoxides in the literature.

3.4.4 Carbon-13 Nuclear Magnetic Resonance Spectroscopy (^{13}C-NMR)

As with FT-IR and Raman spectroscopy, structural characterization of the tin(II) alkoxides by NMR spectroscopy is hindered by their insolubility in organic solvents. High-temperature solution NMR was not available in this work and so their partial solubility in hot solvents such as *o*-dichlorobenzene and DMSO could not be utilized. The only technique which was available to this work was solid-state ^{13}C-NMR at ambient temperature. The ^{13}C-NMR spectra of the tin(II) alkoxides are shown in Figs. 3.17-3.22 with the spectrum of triethylamine hydrochloride shown below in Fig. 3.16 for comparison.

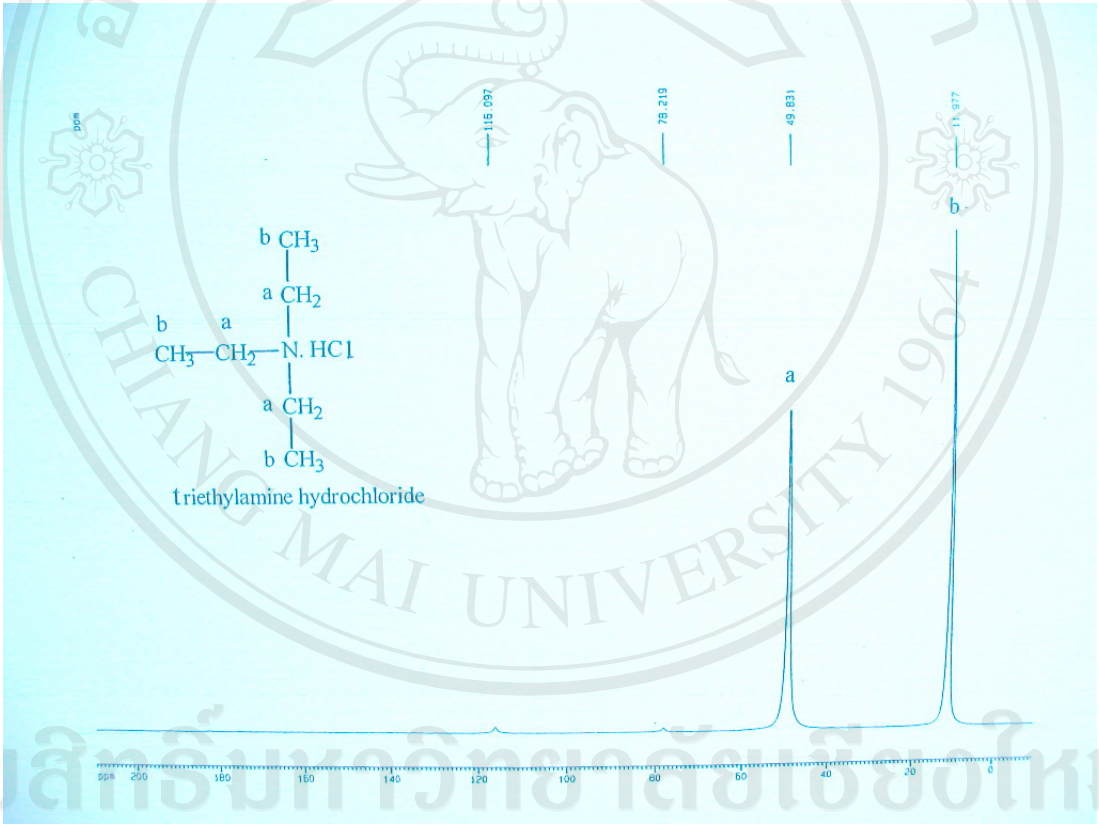

Figure 3.16 Solid-state ^{13}C-NMR spectrum of triethylamine hydrochloride (Commercial product: Sigma).

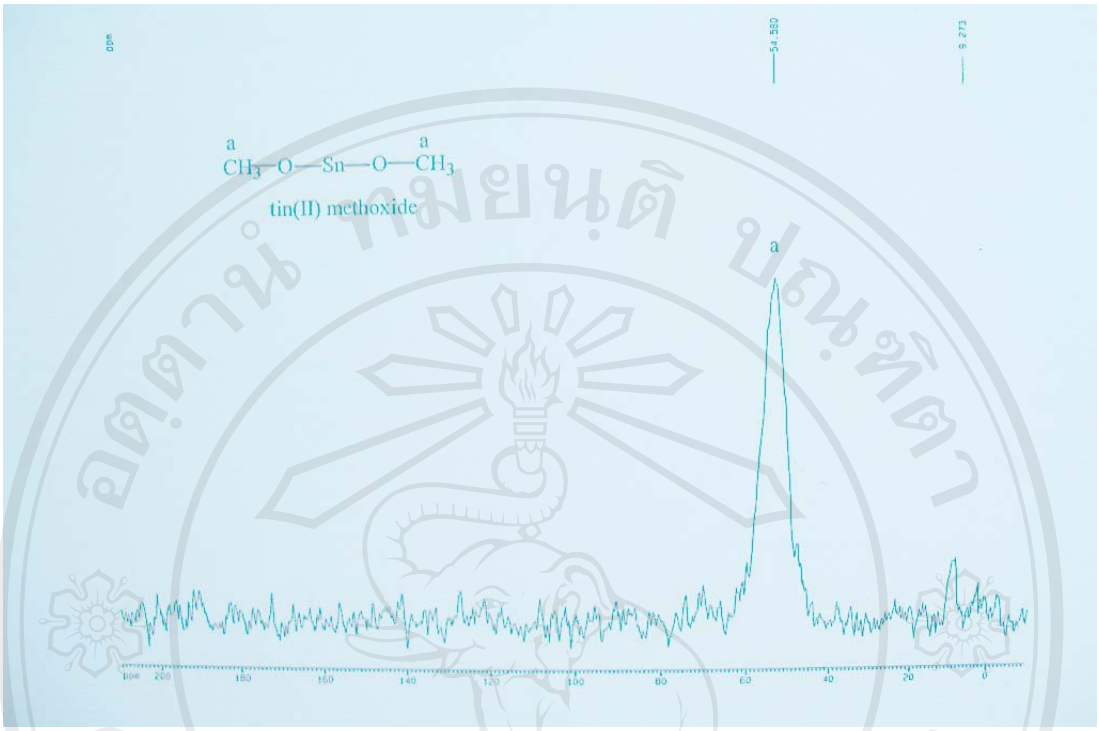

Figure 3.17 Solid-state ^{13}C-NMR spectrum of tin(II) methoxide.

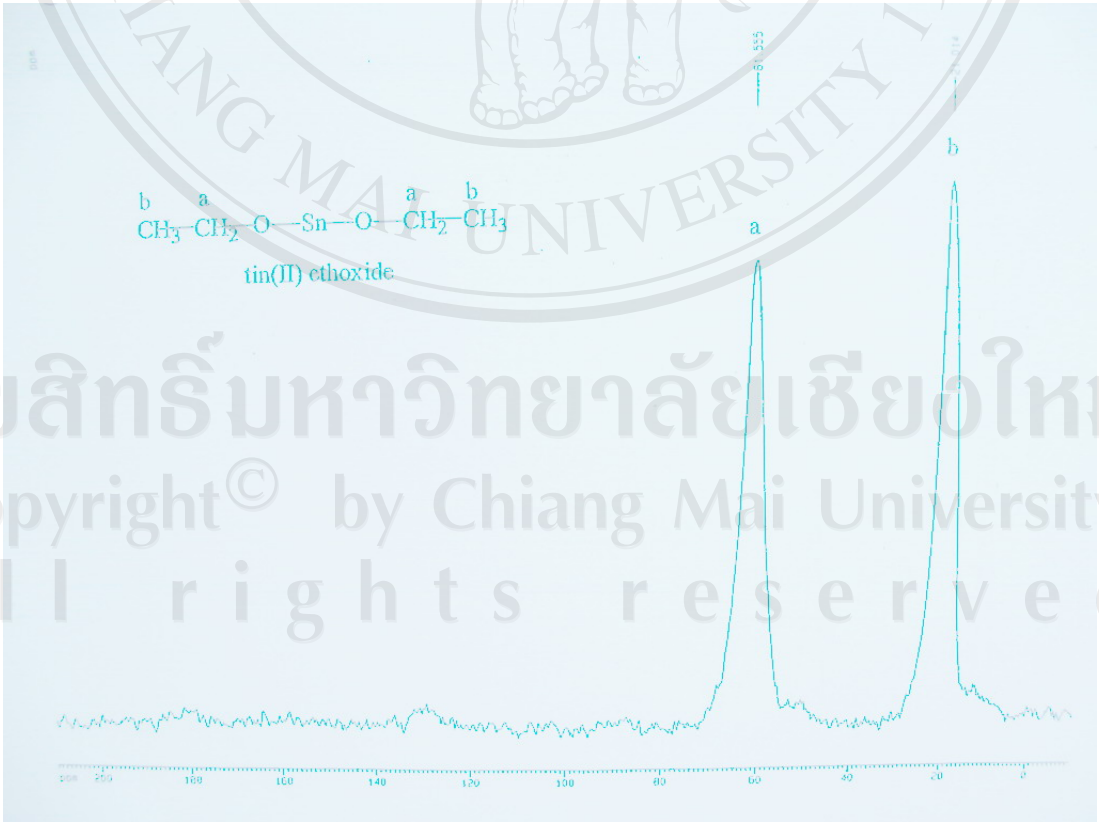

Figure 3.18 Solid-state ^{13}C-NMR spectrum of tin(II) ethoxide.

Figure 3.19 Solid-state ^{13}C-NMR spectrum of tin(II) propoxide.

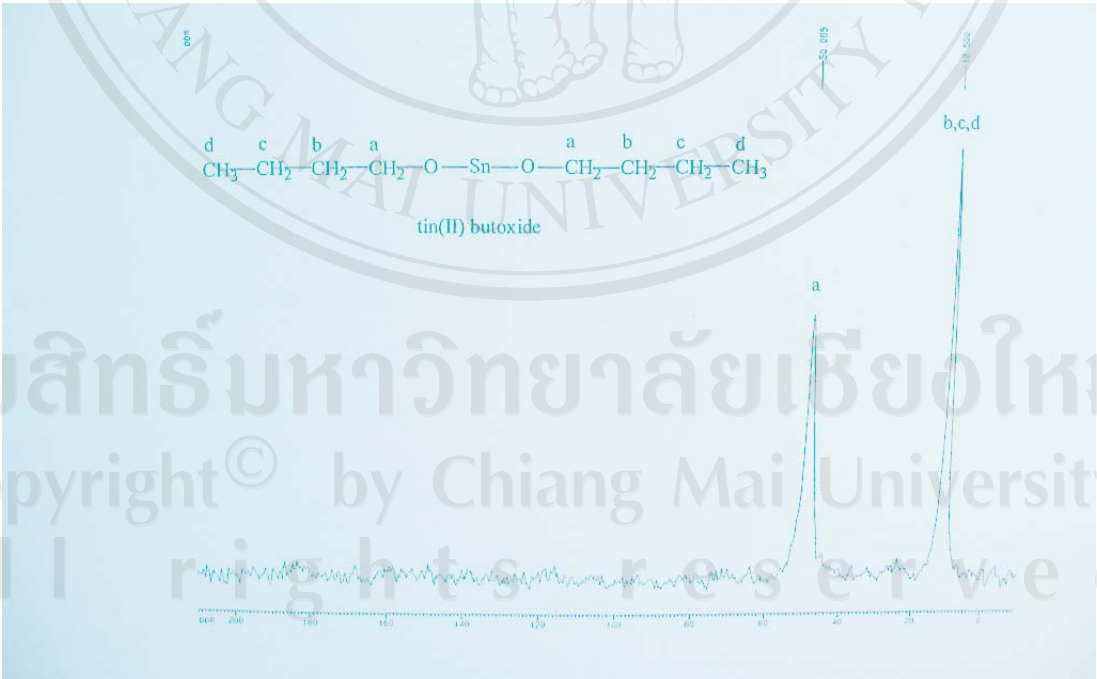

Figure 3.20 Solid-state ^{13}C-NMR spectrum of tin(II) butoxide.

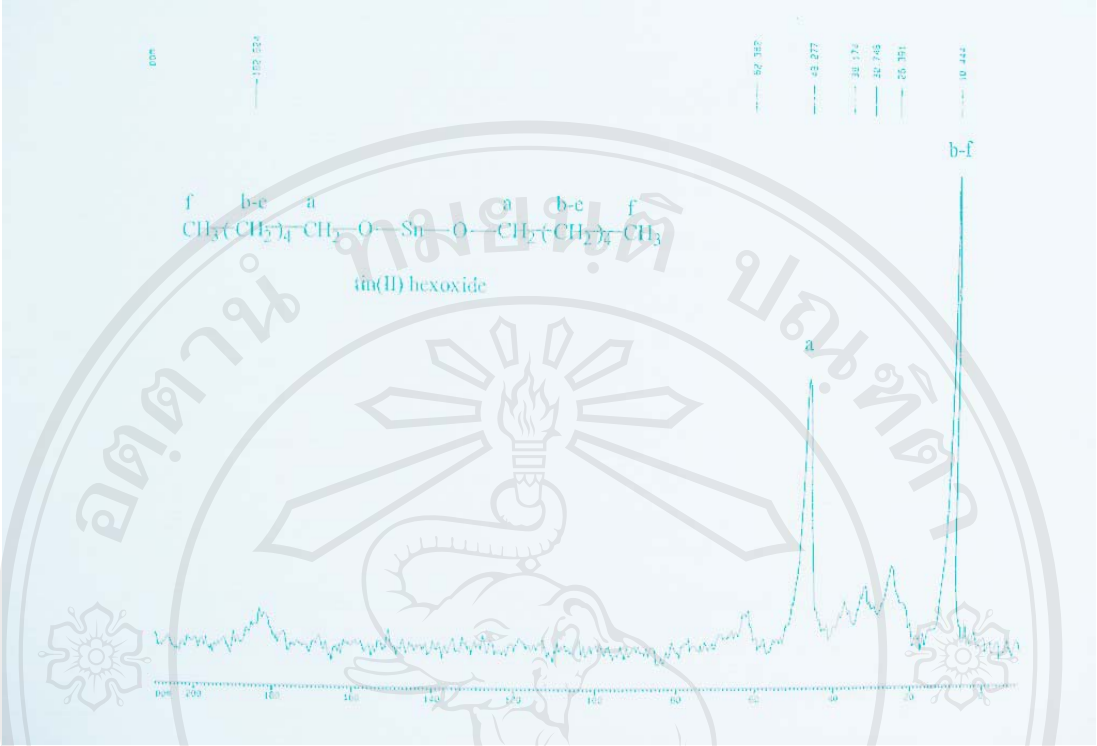

Figure 3.21 Solid-state ^{13}C-NMR spectrum of tin(II) hexoxide.

Figure 3.22 Solid-state ^{13}C-NMR spectrum of tin(II) octoxide.

In common with the Raman spectra, the ^{13}C-NMR spectra of the alkoxides are not as well resolved as was hoped. Compared to triethylamine hydrochloride (Fig. 3.16) which has a stable baseline and narrow sharp peaks, the alkoxides have "noisy" baselines and broad peaks, characteristic of polymeric structures. One noticeable feature of the alkoxide spectra is the upfield shift of about 10 ppm of the peaks for the higher ($R > C_2H_5$) alkoxides. This could be due to a change in the polymeric state from a double oxygen-bridged structure (a) to a more open-chain structure (b), as compared below. Interestingly, these different states were also considered by Gsell and Zeldin [63] to account for differences in their IR spectra below 800 cm^{-1}.

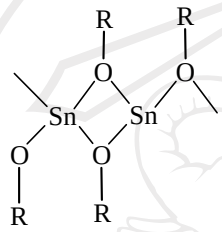

(a) for R = CH_3, C_2H_5

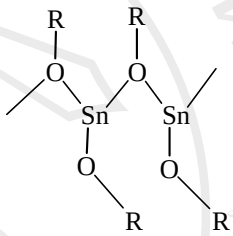

(b) for R > C_2H_5

However, these suggestions remain unconfirmed. More detailed studies are required including, if possible, high-temperature solution NMR in a suitable solvent (or partial solvent) such as *o*-dichlorobenzene or DMSO. Similar to polymers, molecular aggregates need to be broken down by solubilization so that the atoms are less restricted in their atomic motion and are therefore more able to resonate with the applied magnetic field.

3.4.5 Differential Scanning Calorimetry (DSC)

DSC analyses of the tin(II) alkoxide products were conducted at a heating rate of 10.0 ^{o}C/min under a flowing nitrogen atmosphere. Sample weights were typically in the range of 3-5 mg. The DSC thermograms showing the melting endotherms are shown in Figures 3.23-3.28.

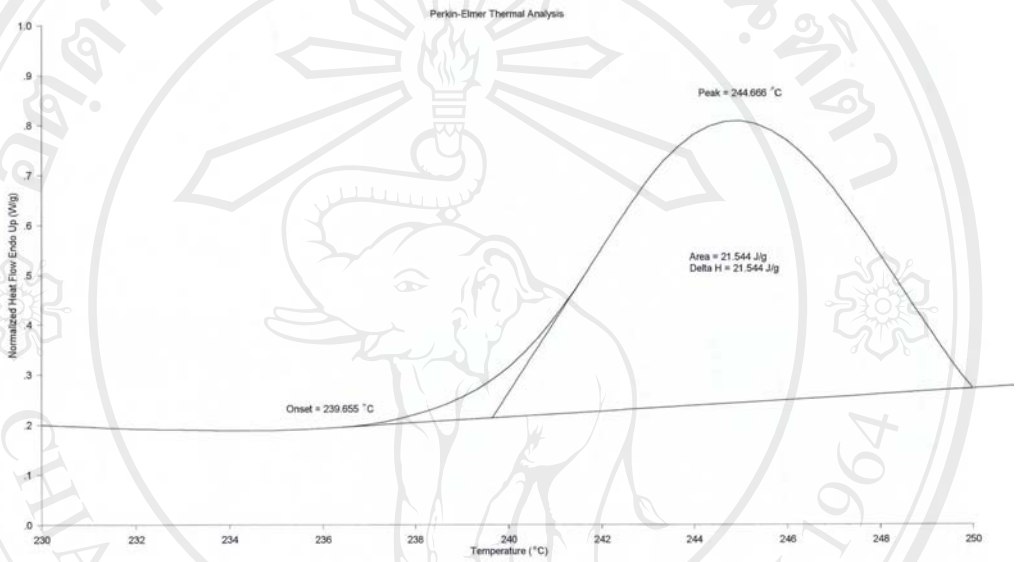

Figure 3.23 DSC melting peak of tin(II) methoxide.

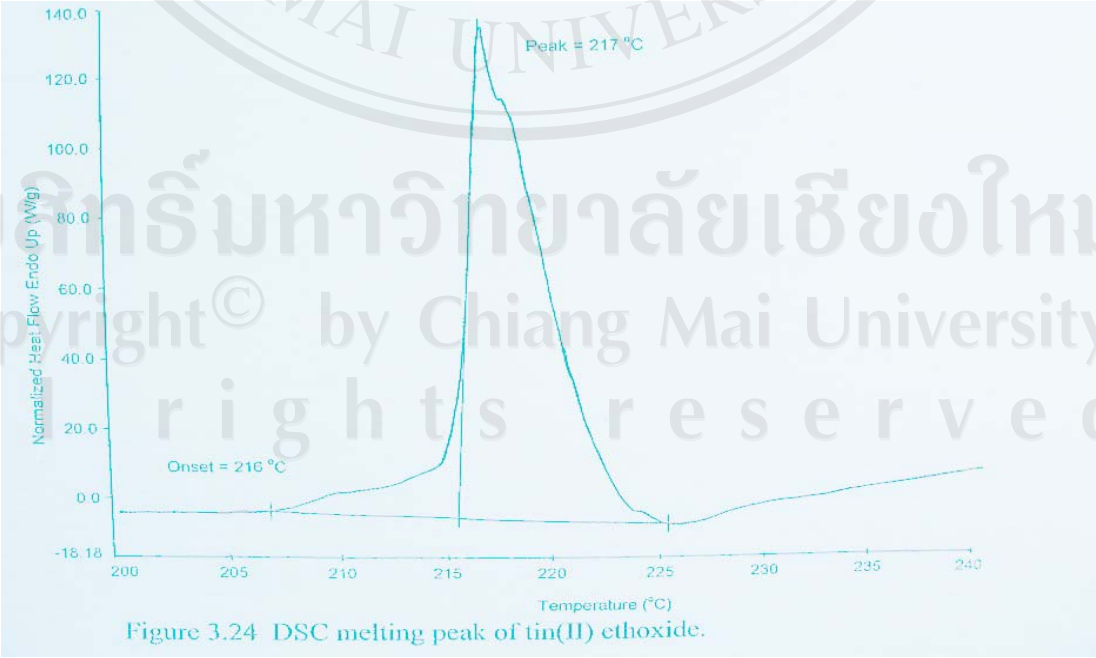

Figure 3.24 DSC melting peak of tin(II) ethoxide.

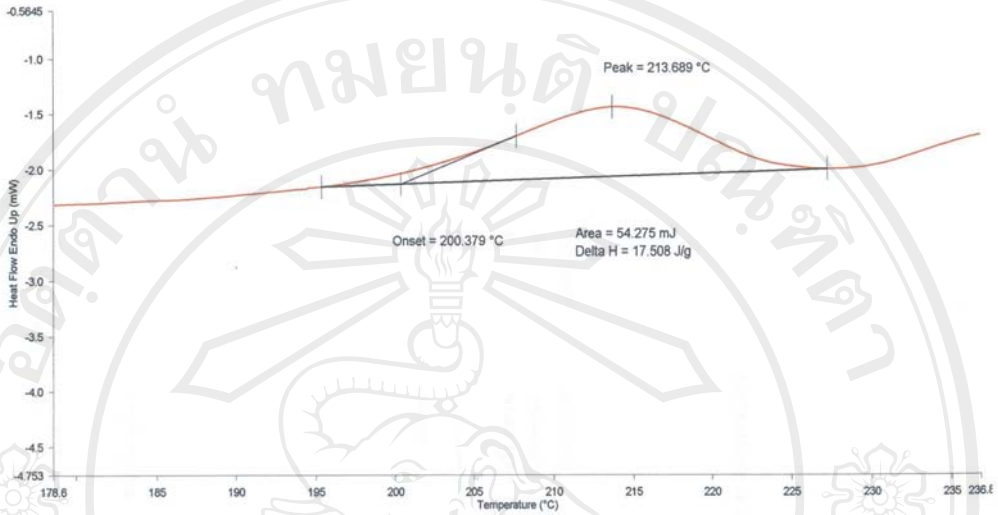

Figure 3.25 DSC melting peak of tin(II) propoxide.

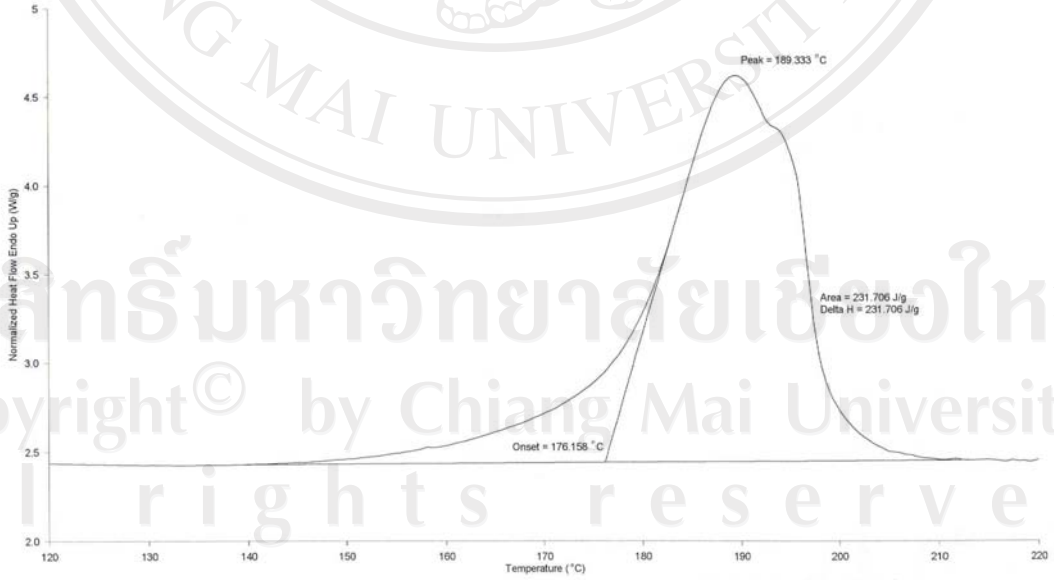

Figure 3.26 DSC melting peak of tin(II) butoxide.

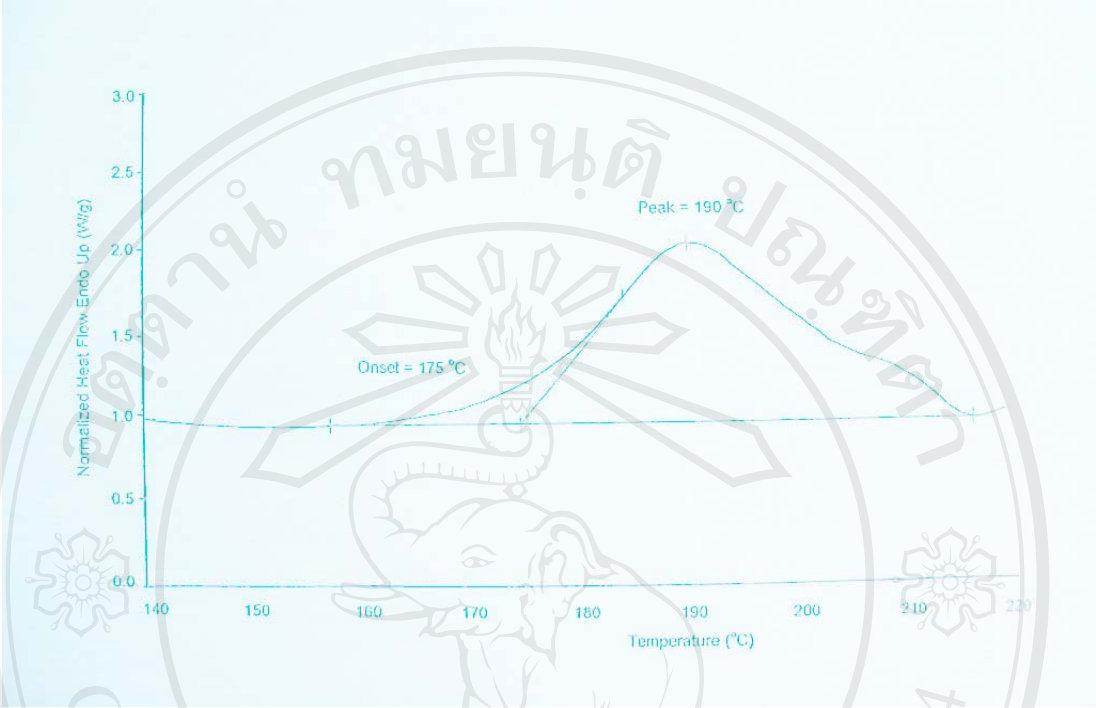

Figure 3.27 DSC melting peak of tin(II) hexoxide.

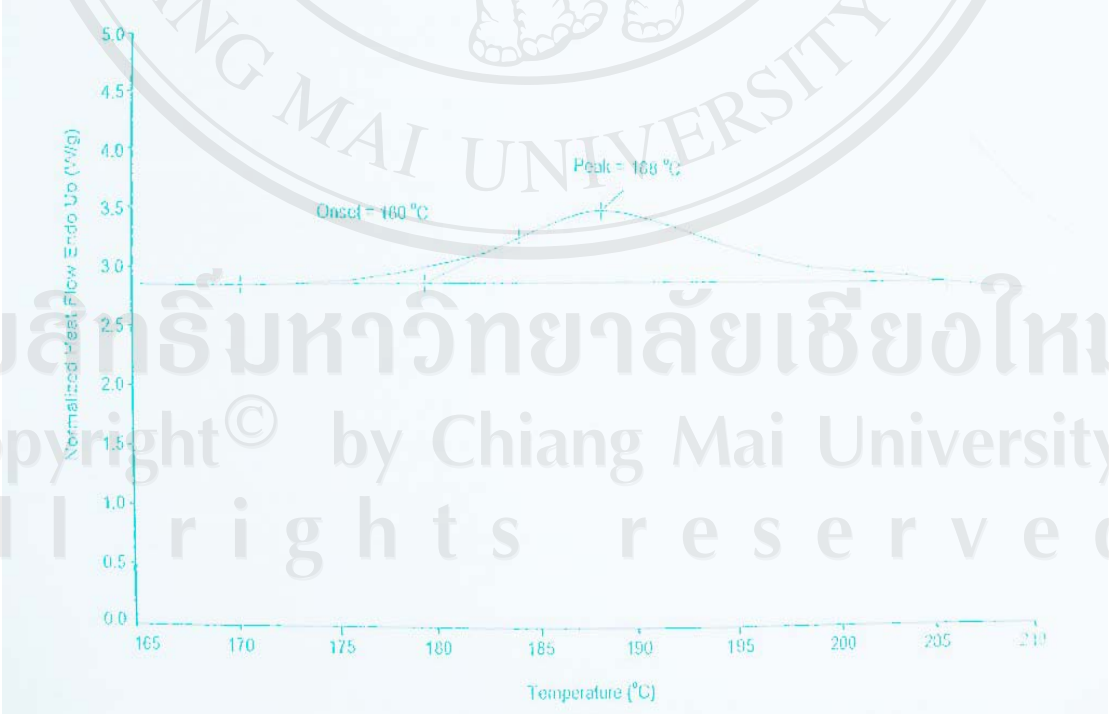

Figure 3.28 DSC melting peak of tin(II) octoxide.

Table 3.16 DSC peak melting temperatures, T_m, of the tin(II) alkoxides compared with reference values from the literature.

Tin(II) Alkoxide	Observed Peak T_m (^oC)	Reference T_m* (^oC)
Tin(II) methoxide	245	242-243
Tin(II) ethoxide	217	> 200 **
Tin(II) propoxide	214	-
Tin(II) butoxide	189	171-172
Tin(II) hexoxide	190	-
Tin(II) octoxide	188	-

* literature values [63]
** decomposes before melting

The melting ranges of the alkoxides are seen to be quite broad, which can be interpreted as another consequence of molecular aggregation. The one exception is the ethoxide in Figure 3.24 which shows a very steep leading edge to the melting peak, a feature which is often associated with samples that thermally decompose as or before they melt. The peak melting temperatures (T_m) from the DSC curves are listed and compared with literature values where available in the above Table 3.16. It is noticeable that, as the alkoxide group increases in length, the T_m decreases. This is as would be expected if the degree and/or strength of molecular aggregation decreases. The melting transition of any chemical compound is a first-order thermodynamic transition and the T_m at which it occurs depends primarily on the energy required to overcome the intermolecular forces of attraction in the crystal. Molecular aggregation enhances these intermolecular forces and, in doing so, increases T_m.

In thermodynamic terms, the value of T_m is given by the equation

$$T_m = \frac{\Delta H_m}{\Delta S_m}$$

where ΔH_m = heat (enthalpy) of melting
ΔS_m = entropy of melting = $S_{melt} - S_{crystal}$

and where both ΔH_m and ΔS_m are positive quantities. Usually, in a series of structurally related compounds in which the variable is a substituent group, as in this series of alkoxides, it is the change in the value of ΔH_m rather than ΔS_m which influences the change in T_m.

3.4.6 Thermogravimetry (TG)

The non-isothermal (dynamic) TG thermograms of the tin(II) alkoxide products were obtained at a heating rate of 20 ^{o}C/min under a nitrogen atmosphere. Sample weights were in the range of 5-10 mg. The TG curves are shown in Figures 3.29-3.34.

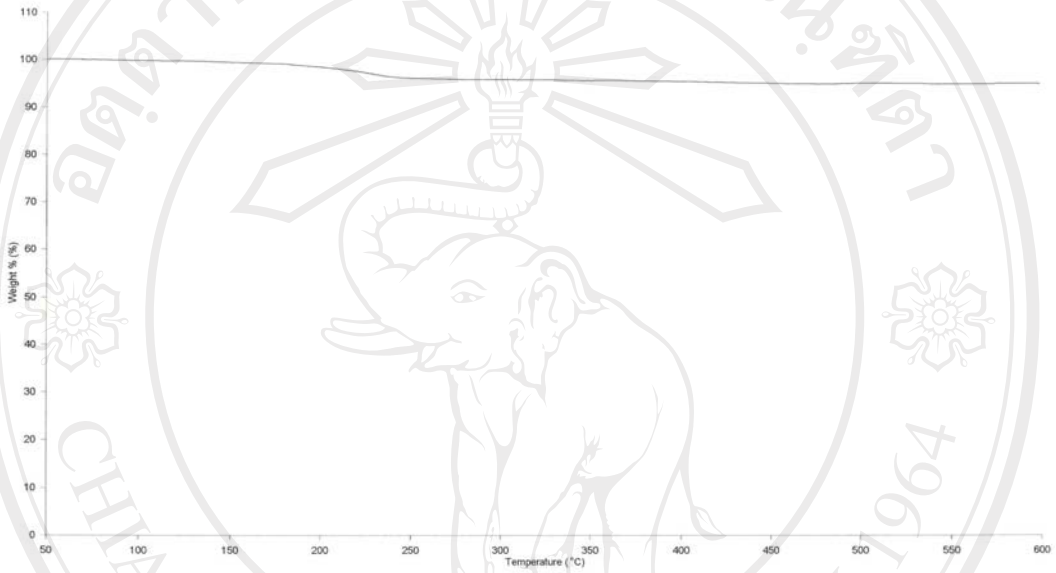

Figure 3.29 Non-isothermal TG thermogram of tin(II) methoxide.

Figure 3.30 Non-isothermal TG thermogram of tin(II) ethoxide.

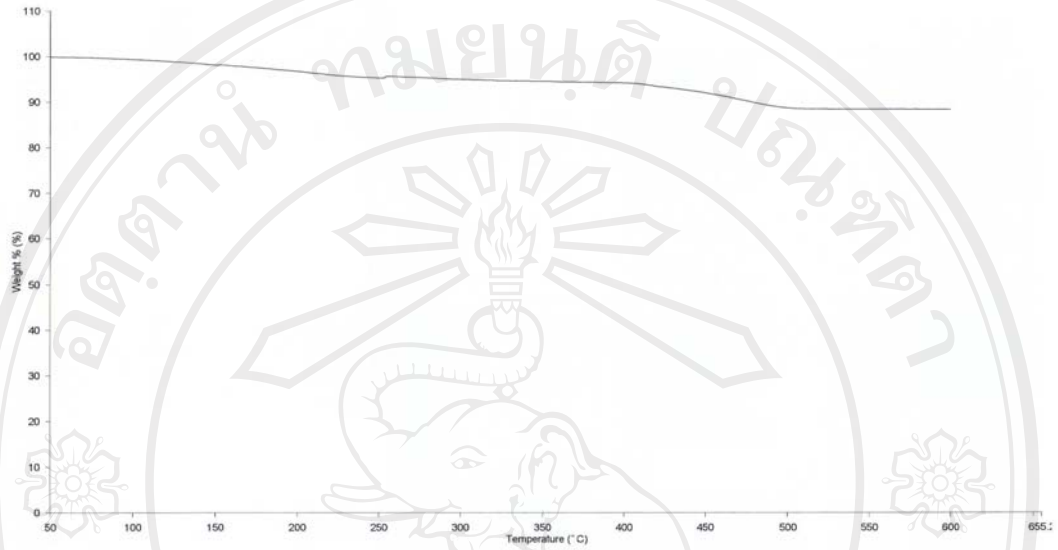

Figure 3.31 Non-isothermal TG thermogram of tin(II) propoxide.

Figure 3.32 Non-isothermal TG thermogram of tin(II) butoxide.

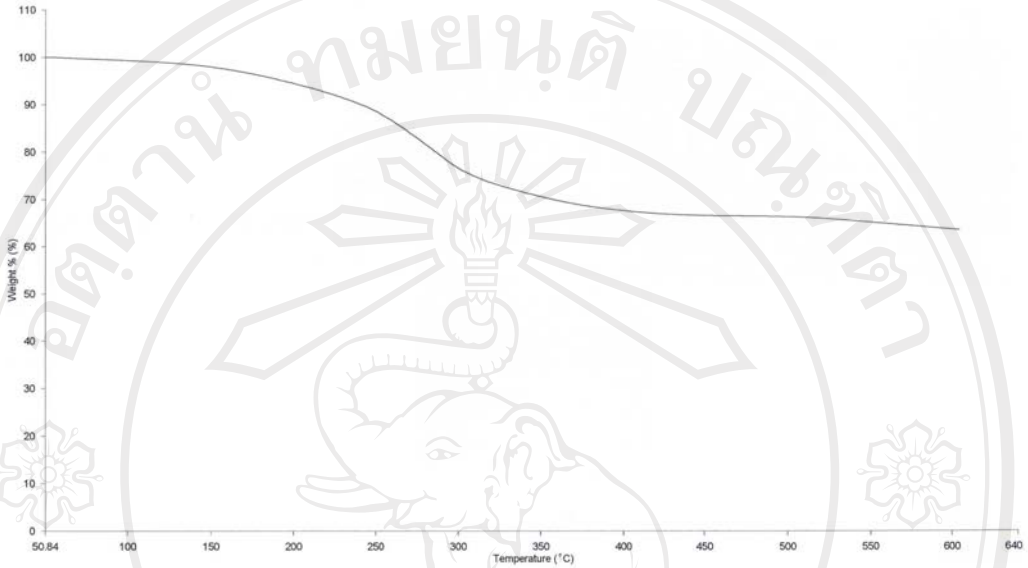

Figure 3.33 Non-isothermal TG thermogram of tin(II) hexoxide.

Figure 3.34 Non-isothermal TG thermogram of tin(II) octoxide.

From these TG curves, it can be seen that thermal stability starts to decline with the butoxide, another observation which corresponds with the apparent decrease in molecular aggregation. Polymeric structures are known to be more thermally stable and this certainly seems to be the case for the methoxide, ethoxide and propoxide, all of which show good thermal stability up to 200 ^{o}C. Another influential factor could be the transition from one polymeric state to another, as mentioned in the previous ^{13}C-NMR section. The double oxygen-bridged form, (a), with its almost "ladder-type" structure, is likely to be more thermally stable than the single oxygen-bridged open-chain form, (b).

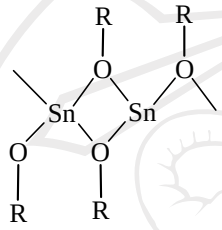

(a)

double oxygen-bridged form

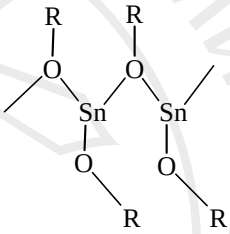

(b)

single oxygen-bridged form

However, the important point as far as this work is concerned is that the alkoxide is thermally stable within the temperature range of 100-150 ^{o}C in which it would normally be used as an initiator in the bulk ROP of cyclic esters. Closer inspection of the TG curves of the butoxide, hexoxide and octoxide shows that their initial weight losses start towards the upper end of this range. This suggests that thermal decomposition might be a problem for these higher alkoxides when used as ROP initiators at higher temperatures.